Since January 2020 Elsevier has created a COVID-19 resource centre with free information in English and Mandarin on the novel coronavirus COVID-19. The COVID-19 resource centre is hosted on Elsevier Connect, the company's public news and information website.

Journal of Molecular Liquids 342 (2021) 116942

Contents lists available at ScienceDirect

Journal of Molecular Liquids

journal homepage: www.elsevier.com/locate/molliq

Molecular docking, DFT analysis, and dynamics simulation of natural bioactive compounds targeting ACE2 and TMPRSS2 dual binding sites of spike protein of SARS CoV-2

Rohitash Yadav [a,*], Shazia Hasan [a], Sumit Mahato [a], Ismail Celik [b], Y.S. Mary [c,*], Ashish Kumar [d], Puneet Dhamija [a], Ambika Sharma [e], Neha Choudhary [f], Pankaj Kumar Chaudhary [g], Ankita Singh Kushwah [g], Jitendra Kumar Chaudhary [h]

[a] Department of Pharmacology, All India Institute of Medical Sciences, Rishikesh, India
[b] Department of Pharmaceutical Chemistry, Faculty of Pharmacy, Erciyes University, Kayseri, Turkey
[c] Thushara, Neethinagar, Kollam, Kerala, India
[d] Department of Biochemistry, All India Institute of Medical Sciences, Rishikesh, India
[e] Department of Biochemistry, U.P. Pt. DeenDayalUpadhyaya Veterinary Science University, Mathura, U.P., India
[f] Centre for Computational Biology and Bioinformatics, School of Life Sciences, Central University of Himachal Pradesh, India
[g] Department of Biotechnology, Indian Institute of Technology, Roorkee, India
[h] Department of Zoology, Shivaji College, University of Delhi, New Delhi, India

ARTICLE INFO

Article history:
Received 1 March 2021
Revised 20 June 2021
Accepted 5 July 2021
Available online 9 July 2021

Keywords:
DFT
MD simulations
SARS-CoV-2
Dual inhibitor
Spike protein

ABSTRACT

The scientific community is continuously working to discover drug candidates against potential targets of SARS-CoV-2, but effective treatment has not been discovered yet. The virus enters the host cell through molecular interaction with its enzymatic receptors i.e., ACE2 and TMPRSS2, which, if, synergistically blocked can lead to the development of novel drug candidates. In this study, 1503 natural bioactive compounds were screened by HTVS, followed by SP and XP docking using Schrodinger Maestro software. Bio-0357 (protozide) and Bio-597 (chrysin) were selected for dynamics simulation based on synergistic binding affinity on S1 (docking score −9.642 and −8.78 kcal/mol) and S2 domains (-5.83 and −5.3 kcal/mol), and the RMSD, RMSF and Rg analyses showed stable interaction. The DFT analysis showed that the adsorption of protozide/chrysin, the band gap of protozide/chrysin-F/G reduced significantly. From SERS, results, it can be concluded that QDs nanocluster will act as a sensor for the detection of drugs. The docking study showed Bio-0357 and Bio-0597 bind to both S1 and S2 domains through stable molecular interactions, which can lead to the discovery of new drug candidates to prevent the entry of SARS-CoV-2. This in-silico study may be helpful to researchers for further in vitro experimental validation and development of new therapy for COVID-19.

1. Introduction

The emergence and spread of a novel corona virus (SARS-CoV-2) from Wuhan city of China to the rest of the world has posed a global health emergency due to its highly contagious nature [1]. The symptoms caused by this virus are similar to previous cases of severe acute respiratory syndrome corona virus (SARS-CoV) and the middle east respiratory syndrome corona virus (MERS-CoV), which outbroke in 2003 and 2012, respectively [2]. SARS-CoV-2 causes severe acute respiratory syndrome (SARS) with an associated mortality of 2%-5% [3–5]. The world health organization (WHO), after careful consideration of the emerging situation, announced it as Public Health Emergency of International Concern (PHEIC) on 30th January 2020 [6]. There are seven strains of human corona viruses, including Alpha corona viruses (229E, NL63) and OC43, HKU1, SARS, MERS, SARS-CoV-2 which are considered as Beta corona viruses [7,8]. Earlier SARS and MERS were the most well-known pathogenic strains accounting for 10% and 36% mortality, respectively, as per the WHO [9].

The SARS-CoV-2, causative agent of COVID-19 (Corona virus disease-19), is a positive sense, single-stranded RNA viruses, encoding two major groups of protein viz., structural and non-structural proteins. The structural proteins include Spike(S), Envelope (E), Nucleocapsid (N), and Membrane (M), and Non-Structural

* Corresponding authors.
E-mail addresses: rohitashyadav1@gmail.com (R. Yadav), marysheena2018@rediffmail.com (Y.S. Mary).

https://doi.org/10.1016/j.molliq.2021.116942
0167-7322/

proteins entail nsp1 through nsp16 [10]. These structural and non-structural proteins are being assessed as potential targets for novel drugs as no specific, safe and effective drugs are available for SARS-CoV-2 till date. Therefore, researchers are actively engaged in identifying potential target proteins for drug discovery by employing myriad of tools and techniques. Besides, multiple FDA-approved drugs, including Chloroquine, Hydroxychloroquine, Lopinavir, Favipiravir, Ivermectin, Ritonavir and Remdesivir, are also being repurposed/repositioned for the COVID-19, however, their clinical outcomes have reportedly been variable, necessitating new drug (s) with consistent effectiveness and specificity [11].

In recent times, *in silico* analysis is considered as one of the suitable and fastest approaches to screen the innumerable number of therapeutic molecules and/or drugs in order to discover the new drug for emerging diseases. Therefore, recently, numerous *in-silico* docking studies were carried out and published, primarily targeting the spike (S) protein [12,13], main protease [14–19], N protein [20–23], and RNA-dependent RNA polymerase amongst others. Despite consistent scientific efforts around the world to contrive potential drug molecules, antibody cocktails, and vaccines against potential targets of this tiny virus, there have not been successful findings of the effective drug candidate for COVID-19 till date. During SARS-CoV-2 infection, the crucial role is played by two types of protein domains/subunits, S1 and S2, present on membrane-bound spike protein. The S1 plays an important role during initial attachment and entry of the virus to the host cells through Receptor Binding Domain (RBD) [24], and thereafter, it tends to dissociate whereas, S2 achieves a more stable fusion state through conformational transitioning [25]. The human Angiotensin-Converting Enzyme 2 (hACE2) binds to the RBD, located on S1 subunit (RBD/S1) of the homotrimeric spike proteins and TMPRSS2 plays an important role in the cleavage of S1/S1 subunits responsible for viral entry in the human host cell [26]. Nanoclusters, like fullerene and graphene are potential candidates to build a new generation of sensors and drug carriers [27]. Many drug adsorption studies of nanoclusters have recently been reported [28,29].

Considering above mentioned fact, this study claims to identify promising drugs that can synergistically block the interaction of ACE2 and TMPRSS2 on S1 and S2 domains of spike protein hotspots, and thus may prevent the entry and fusion of SARS-CoV-2. The systematic drug repurposing of bioactive compounds was done with molecular docking and molecular dynamics simulations. The parameters calculated include estimated docking score, intermolecular hydrogen bonds (HB), Root Mean Square Deviation (RMSD), Root Mean Square Fluctuation (RMSF), and Radius of Gyration (Rg).

2. Material and methods

2.1. Target selection and protein & ligand preparation

The purpose of this study was to obtain detailed information regarding the newly hypothesized receptor on human cells, ACE2, which interacts with corona virus surface proteins to establish viral infection. The three-dimensional crystal structure of SARS-CoV-2 spike glycoproteins (PDB IDs: 6XR8) was retrieved from the RCSB protein data bank (https://www.rcsb.org/structure/6XR8). The downloaded protein was further prepared by using Schrodinger's protein preparation wizard in which we have removed the undesired protein's subunits, het atoms, and water molecules [30]. Chain A of spike protein was taken for further preparation. It corrected the structure by adding hydrogen atoms to the source structure. Additionally, the OPLS3e force field was utilized for optimizing protein energies and removing steric hindrance. A total of 789 compounds were used from the IBS Intra-BioScreen compounds database. The 2D structures of potential ligands were downloaded and prepared for docking study. The ligands were prepared by using the Ligprep module with suitable parameters like optimization, tautomers, ring conformation, 2D to 3D conversion, determination of promoters, ionization states at pH 7.0 with partial atomic charges using OPLS3e force field A [30].

2.2. Receptor grid generation and active ligand binding Site prediction

The most important aspect of the computational docking of the novel chemical entities is to identify and recognize the binding site of the target protein structure. The active site of 6XR8 contains hydrophobic and hydrophilic regions with hydrogen donors and acceptors. The active ligand binding sites for receptor-ligand binding interaction of spike protein (pdb id: 6XR8) were predicted using sitemap modules of the Schrodinger suite [31]. The receptor grid box was generated using the grid generation module of the Schrodinger suite by preferring active site residues after their prediction. The atoms of protein were fixed within the default parameters of the radii of Van der Waal's scaling factor of 1 Å with a partial charge cut-off of 0.25 Å using the OPLS3e force field and 20 Å docked ligand length. The dimensions of the receptor setup and grid box werex = 10 Å, y = 10 Å, z = 10 Å and × = 20 Å, y = 20 Å, z = 20 Å, respectively with1 Å grid box space [32].

2.3. Virtual screening and ligand–protein docking

The virtual screening process involves three main steps (Fig. 1). The first step was the high throughput virtual screening (HTVS) mode employed for structural conformation of all the 1503 ligands used in this study. The second step was 375 (25% of HTVS) ligands were screened by the SP docking process. The third step was to finalize the 100 (25% of SP docking) compounds based on their binding affinity to the XP docking protocol. The same procedure was followed for docking with Site-2 and Site-3. Finally, the top ten ligands were selected from Site-1, Site-2, and Site-3. The algorithm used in molecular docking by Standard Precision (SP) and Extra Precision (XP) has proved to be an accurate and reliable one [33]. It is generally used to explore the protein–ligand interactions in terms of their hydrogen bond interactions, Van der Waals (vdW) forces, hydrophobic interactions, and π-π interactions. It can also reflect other aspects of protein–ligand interactions, including corresponding binding free energies.

2.4. Protein-protein docking

The ClusPro2.0 server (http://ClusPro.bu.edu/) was used to predict the possible interaction between two different protein structures. Table 1 shows the properties of the protein structure of spike protein, ACE2, and TMPRSS2. The chain-A of spike protein structure (PDB ID: 6XR8) docked with chain D of ACE2 (PDB ID:7A92) and modeled structure TMPRSS2 were submitted to the ClusPro server. Each cluster is characterized by its number of members, the ClusPro score of the center of the cluster, and the lowest ClusPro score found in the cluster. The balanced ClusPro score was used for possible interaction prediction between docking proteins. For each monomeric input, we kept the dimeric solution presenting the lowest ClusPro score. For the determination of the interactions at the interface of the protein–protein complex, the Protein Interaction Calculator (PIC) was used, which helped to determine the various interactions at the interface of the dimers [34]. Predictive interactions residues involved in hydrophobic contacts, salt bridges, and hydrogen bonds were identified.

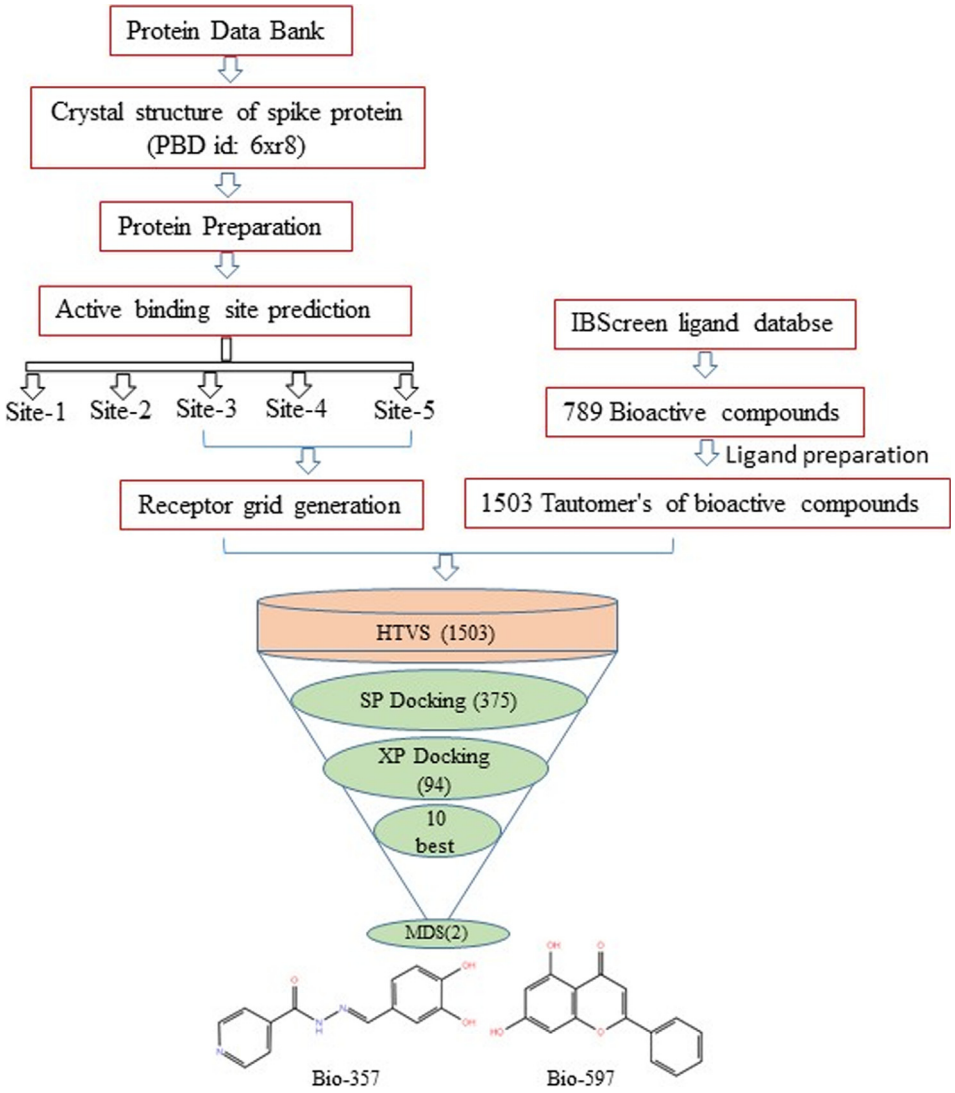

Fig. 1. Virtual screening and docking workflow. HTVS (High throughput virtual screening); SP (Standard precision); XP (Extra precision); MDS (Molecular dynamics simulation).

Table 1
Three dimensional structures of spike protein, ACE2 & TMPRSS2, and their properties.

Protein structure	PDB ID	Method	Resolution	Sequence length	Number of chains
Spike glycoprotein	6XR8	Electron Microscope	2.90 Å	1310	A,B,C
ACE2	6M0J	X-RAY DIFFRACTION	2.45 Å	603	A

2.5. Molecular dynamics simulation

Molecular dynamics simulation (MDS) was performed using the Gromacs 2020.4 version [35]. Missing atoms and residues in protein structure were completed with Swiss PDB Viewer [36]. The protein of 1148 residues and ligand topology were created with pdb2gmx and CGenFF server and Charmm36-Jul2020 force field, respectively [37]. It was minimized by solvation with the TIP3P water model, and 6Na+ ions were added. The total system energy was minimized by the protein–ligand complex Canonical ensemble (amount of substance (N), pressure (P) and temperature (T) - NVT) and Isothermal-isobaric (amount of substance (N), volume (V), and equilibrium steps temperature (T) - NPT) were carried out at 100 ps. Molecular dynamics of 10 ns duration were run. Root mean square deviation (RMSD), Root mean square fluctuation (RMSF), Radius of gyration (Rg), hydrogen bond analyses between protein and ligand were calculated.

2.6. DFT analysis

For modelling protozide and chrysinon on fullerene and graphene, all the structures are optimized independently (Fig. 2). To find protozide/chrysin-F/G interaction, (initially, protozide/chrysin is put in a parallel position with F/G), wB97xD/6-31G* level was used with Gaussian09 and Gaussview [38,39]. The adsorption energy (E_{ad}) calculation of protozide/chrysin-F/G is as by Almuqrin et al. [40].

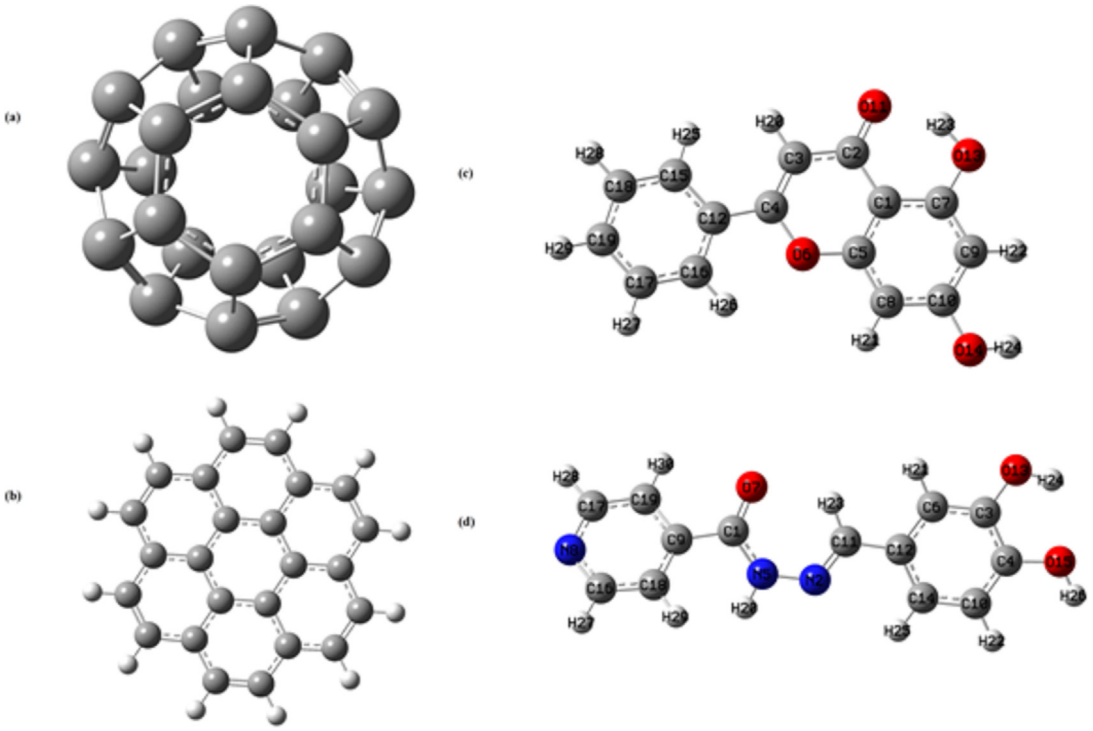

Fig. 2. Optimized structures of (a) fullerene (b) graphene (c) chrysin (d) protozide.

3. Results and discussions

3.1. Protein structure reliability and active site selection

The PROCHECK server was used to generate a Ramachandran plot displaying allowed and disallowed regions (https://servicesn.mbi.ucla.edu/PROCHECK/) [41]. It needs more than 90% residues in the most favored region to be a standard model of good quality and reliability of three-dimensional structures. The protein structure used in this study (6XR8) has 92.3% residues in the most favored region and the rest 7.7% are in the additional allowed regions (Fig. S1-Supporting information). Therefore, the structure used in our study is reliable as 100% of the residues lie in allowed regions. Since the disallowed regions are generally involved in steric hindrance, therefore, this plot shows minimum steric interactions and good stereo chemical quality of 3D protein structure. The active binding pockets on spike protein were predicted using the Sitemap tool of Maestro 12.4 version of Schrodinger software (Table 2). Total five active sites were predicted (Fig. S2), among them site1 was found on S1 subunit with associated residues involving Leu18, Ala243, Leu244, Ser254, Ser255, Gly257, Trp258, Thr259, Ala260, Gly261, Ala262, I Le68, Hie69, Ly597, Ser98, Asn99, Ile100, Phe140, Val143, Tyr144, Tyr145, Trp152, Glu156, Arg158, Leu179, Gly181, Lys182, Gln183, Gly184. The Site-2 was predicted on fusion peptide (788–806) and HR1(912–984) of S2 subunit, and associated residues are Val729, Ser730, Met731, Thr732, Lys733, Gln774, Asp775, Thr778, Phe782, Phe823, Ala831, Gly832, Phe833, Leu861, Pro862, Pro863, Leu864, Leu865, Thr866, Asp867, Ile870, Ser1055, Ala1056, Pro1057, Hie1058, Gly1059. The site-3 was predicted on receptor binding domain of S1 subunit of spike protein, and active site residues of site-3 are Cys336, Pro337, Phe338, Val341, Phe342, Ile358, Ala363, Tyr365, Leu368, Tyr369, Ala372, Phe374, Phe377, Leu387, Phe392, Val395, Cys432, Ile434, Leu513, Phe515, Val524. Site 3 and 4 were predicated on the S1 subunit and HR1 & HR2 of the S2 subunit but both sites were excluded from the study due to less than one DScore. Three receptor grids were generated on site1, 2, and 3 using the associated active site residues for the docking study.

Table 2
Dscore, size and active site residues of 6xr8 predicted by Schrodinger's sitemap tools.

S/N	Active Site	DScore	Residues
1	Site-1	1.00	Leu18, Ala243, Leu244, Ser254, Ser255, Gly257, Trp258, Thr259, Ala260, Gly261, Ala262, I Le68, Hie69, Ly597, Ser98, Asn99, Ile100, Phe140, Val143, Tyr144, Tyr145, Trp152, Glu156, Arg158, Leu179, Gly181, Lys182, Gln183, Gly184
2	Site-2	1.09	Val729, Ser730, Met731, Thr732, Lys733, Gln774, Asp775, Thr778, Phe782, Phe823, Ala831, Gly832, Phe833, Leu861, Pro862, Pro863, Leu864, Leu865, Thr866, Asp867, Ile870, Ser1055, Ala1056, Pro1057, Hie1058, Gly1059
3	Site-3	1.468	Cys336, Pro337, Phe338, Val341, Phe342, Ile358, Ala363, Tyr365, Leu368, Tyr369, Ala372, Phe374, Phe377, Leu387, Phe392, Val395, Cys432, Ile434, Leu513, Phe515, Val524.
4	Site-4	0.9	94, 96, 99, 101, 102, 103, 104, 119, 121, 126, 128, 177, 190, 192, 194, 203, 226, 227
5	Site-5	0.8	907, 910, 911, 912, 914, 1091, 1092, 1093, 1104, 1105, 1106, 1107, 1108, 1111, 1113, 1119

3.2. Protein-ligand docking

Three binding pockets (Site1, 2, and 3) on S1 and S2 subunits of spike proteins were selected for screening and docking of 1503 bioactive Phyto-compounds. After high throughput virtual screen, 25% (375 ligands) ligands were used in standard precision and 25% (95 ligands) of SP docking were used for XP docking. Finally, the best 10 ligands were finalized for further study based on the lowest docking score (Table 3). Magnolol, Curcumin, Protozide, Auraptene, Acitretin, Fosenazide, Chrysin, Alizarin, GT-44, and Aripiprazole were top 10 ligand molecules and their docking score

Table 3
Docking Results of Bioactive Phyto-compounds Compounds from ibscreen database against site 1, 2 & 3 1.46 of 6XR8 target protein.

	Site-3 (DScore 1.46)		Site-2 (DScore 1.09)		Site-1 (DScore 1.00)	
S/No	Compound ID	Docking Score	Compound ID	Docking Score	Compound ID	Docking Score
1	Bio-0675	−10.38	Bio-0174	−6.73	Bio-0613	−6.85
2	Bio-0677	−9.85	Bio-0043	−6.53	Bio-0109	−6.34
3	Bio-0357	−9.642	Bio-0287	−6.42	Bio-0312	−6.18
4	Bio-0625	−9.592	Bio-0924	−5.96	Bio-0034	−6.12
5	Bio-0002	−9.577	Bio-0597	−5.83	Bio-0219	−6.02
6	Bio-0437	−9.153	Bio-0617	−5.63	Bio-0247	−5.79
7	Bio-0597	−8.78	Bio-0640	−5.45	Bio-0047	−5.78
8	Bio-0224	−8.678	Bio-0357	−5.30	Bio-0594	−5.76
9	Bio-0385	−8.649	Bio-0369	−5.19	Bio-0444	−5.71
10	Bio-0004	−8.632	Bio-0808	−5.18	Bio-0357	−5.69

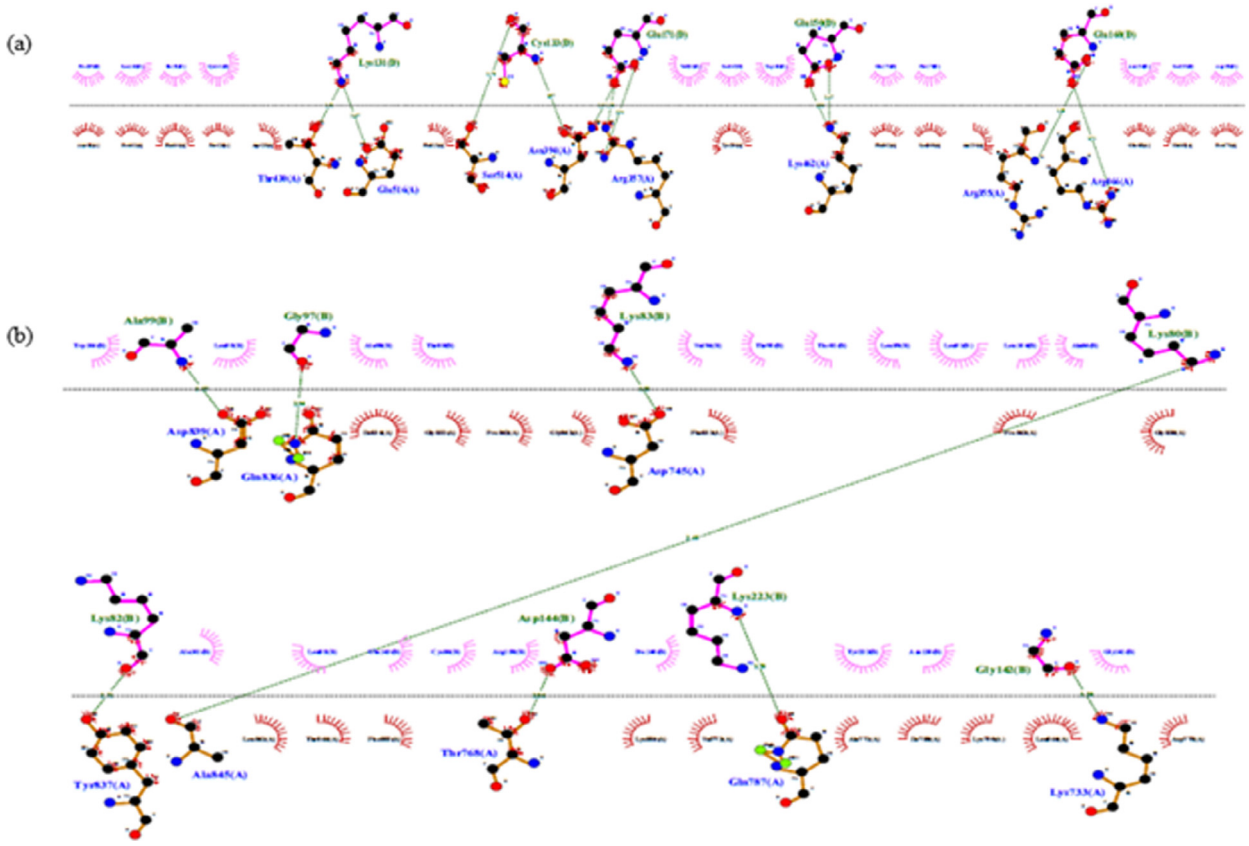

Fig. 3. Physiochemical interactions of protein–protein docking complex. A) protein–protein. Docking interactive residues between spike protein and ACE2. B) Protein-protein docking interactive residues between spike protein and ACE2 with TMPRSS2.

are −10.38, −9.85, −9.642, −9.592, −9.577, −9.153, −8.78, −8.678, −8.649, −8.632 respectively. These ligands predicted to be able to interact with the receptor-binding site of spike protein, thereby excluding the possibility of virus binding with ACE2 receptor and entry in the host cell. Interactive residues of these ligands are Ser373, Tyr369, Phe374, and Leu387. Bio-0174, Bio-0043, Bio-0287, Bio-0924, Bio-0597, Bio-0617, Bio-0640, Bio-0357, Bio-0369, Bio-0808 are best ten ligands docked with S2 subunit, and docking score are −6.73, −6.53, −6.42, −5.96, −5.83, −5.63, −5.45, −5.30, −5.19, −5.18, respectively. Protein-ligand interactive residues on S2 subunits are Asp867, Pro863, Ser730, Thr778, Ser730, Thr778, Thr778, Gly1059, Ala1056, Ser730, Ser730, Asp867, and Gly832. Molecular docking analysis of several plant compounds against S protein (6VXX) and M^{pro} (6LU7) gives binding free energies in the ranges −10.4 to −5.5 and −8.3 to −5.3 kcal/mol [42].The phytochemical emodin binds with spike protein fragment and its receptor human ACE2 protein similar to that of hesperidin but its binding energy −6.19 kcal/mol is less than that of hesperidin (-8.99 kcal/mol) [43].

TMRPSS2 binds with the S2 subunit, thereby facilitating molecular interaction between receptor binding domain and human ACE2, and eventually cleaves between S1/S2 subunit of the spike protein. Bio-0613, Bio-0109, Bio-0312, Bio-0034, Bio-0219, Bio-0247, Bio-0047, Bio-0594, Bio-0444, Bio-0357 are the best ten ligands docked with site 1 associated S1 subunit residues including, Hie69, Leu179, Ser98, Val143, Thr259, Leu244, Val143, Glu156, Ser254, Gly181, Ala262, Tyr145, Gly257. Docking score of all ten ligand compounds are −6.85, −6.34, −6.18, −6.12, −6.02, −5.79, −5.78, −5.76, −5.71, and −5.69, respectively.

Ligand Bio-0357 binds with both S1 and S2 subunits with all three active sites (Site 3, 2, and 1) with good docking score (-9.642, −5.30 and −5.69, respectively) (Table 3). Whereas ligand Bio-0597 binds both subunits through Site 3 and 2, and docking scores are −8.78 and −5.83 with site 3 and 2, respectively (Table 3).

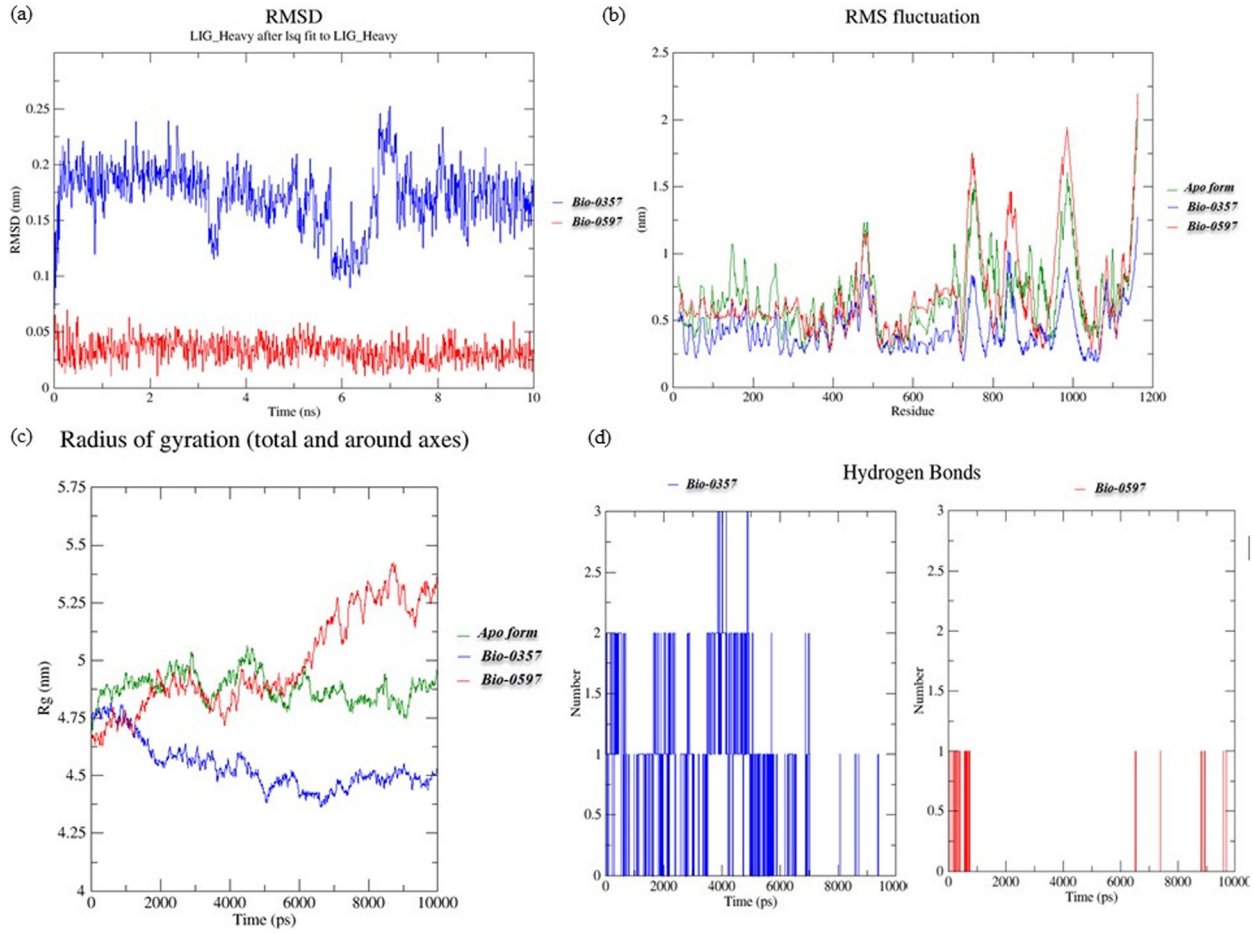

Fig. 4. (a) Root Mean Square Deviation (RMSD) of ligand protein complex of Bio-0357, Bio-597 and apo form for 50 ns. (b) Root Mean Square Fluctuation (RMSF) of ligand protein complex of Bio-0357, Bio-597 and apo form for 50 ns. (c)Radius of gyration (Rg) shows the ligand–protein complex of Bio-0357, Bio-597 and apo form for 50 ns. (d) The number of Intermolecular H bonds between the ligands (Bio-375 & Bio-597) and amino acid residues of SARS CoV-2 spike glycoprotein (pdb id: 6xr8) during 50 ns.

Previously ivermectin and remdesivir have been reported the binding affinity with spike protein and TMPRSS2 [44].Binding affinity of ivermectin with spike protein found to be docked between the viral spike and the ACE2 receptor. The molecular docking of ivermectin with TMPRSS2 suggested an important role of ivermectin in inhibiting the entry of the virus into the host cell, probably by increasing the endosomal pH [45].Hoffmann et al., reported that remdesivir showed high affinity to spike but formed unstable complex, however, it showed considerable high affinity to both TMPRSS2 and ACE-2 might denote its possible roles in blocking cellular receptor necessary for viral entry in addition to inhibiting TMPRSS2 induced membranes' fusion required for the SARS-CoV-2 replication [26].

Figs. S3 and S4 show the physicochemical interaction of ligand–protein complex of Bio-0357 and Bio-597 with S1 (site-3), and S2 (Site-2) subunit of spike protein, respectively, whereas Fig. S5 shows the physicochemical interaction of ligand Bio-0357 with S1 subunit (Site-1). Interestingly, ligand Bio-0357 can block the activity of TMPRSS2 through the S2 subunit and may also inhibit the fusion of the S1 subunit with ace2 by blocking the receptor-binding domain of spike protein. The chemical structure and biological activity of both selected and therapeutically promising molecules are mentioned in Table S1 (supporting information).

3.3. Protein-protein docking

Attachment and proteolytic cleavage of the viral spike protein, resulting in the formation of two fragments, S1/S2 and S2′ by host ACE2 and TMPRSS2, are pre-requisite for viral entry into the host cell [26]. The cleavage at the later site results in the production of S1/S2 and S2′ fragments required for the viral entry into the cells [46]. This provides an excellent basis on which docking simulations could be directed. Therefore, in this study, we analyze protein–protein interaction between spike protein and ACE2 and TMPRSS2 using the ClusPro2.0 server. Fig. 3-(a) and (b) show the interactive residues of spike protein with ACE2 and TMPRSS2 protein–protein docking complex. The Thr430-Lys131, Glu516-Lys131, Ser514-Cys133, Asn394-Cys133, Asn394-Glu171, Arg357-Glu171(2x), Lys462-Glu150(2x), Arg355-Glu160, ARG466-Glu160 are the interactive residues between the S1 subunit of spike protein and ACE2 docking complex. The Asp839-Ala99, Glu836-Gly97, Asp745-Lys83, Tyr837-Lys82, Ala845-Lys80, Thr768-Asp144, Glu787-Lys223, Lys733-Gly141 are the interactive amino acids between the S2 domain and TMPRSS2.

3.4. MD simulations

Molecular dynamics simulation studies of 50 ns duration were carried out to further analyze the interactions of the complex structure formed with the SARS-CoV-2 spike glycoprotein (PDB: 6XR8) and Bio-0357 and Bio-597, which gives the lowest value according to the docking score. To validate the molecular dynamics system, the spike protein was simulated with apo without ligand. RMSD measurement of the complex structures according to the ligand was performed. As shown in Fig. 4(a), Bio-0357, Bio-0597, and spike complex structures showed an RMSD value between

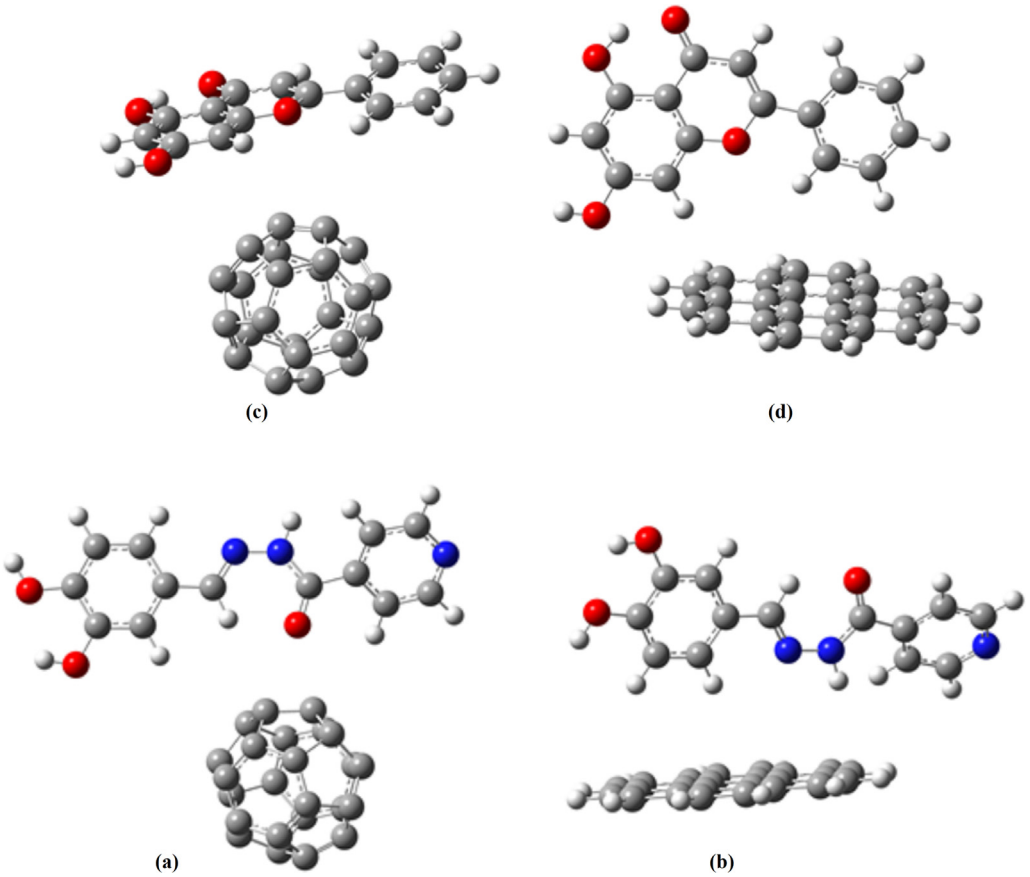

Fig. 5. Optimized structures of (a) protozide-F (b) protozide-G (c) chrysin-F (d) chrysin-G.

0.1 and 0.25 nm, and below 0.075 nm, respectively. Bio-0597 exhibited a lower RMSD profile than the Bio-0357 compound. Accordingly, the Bio-0597 and Bio-0357 compounds formed a stable and consistent structure with the spike protein. In this case, it was seen that the ligand structures are stable, and the stability of complex compounds was high.

The fluctuation of protein structures was calculated on a residue basis by selecting 'c-alpha'. As shown in Fig. 4(b), the RMSF value of the apo form and protein–ligand complex structures were measured below 2 nm. Following RMSF graph examination, it was determined that Bio-0357 had less fluctuation and a more stable structure compared to apo form and Bio-0597. In contrast, Bio-0597 showed less fluctuation than the apo form until the 720th residue, but higher fluctuation than the apo form was measured. Also, Bio-597 exhibited the highest fluctuation at 1.92 nm. Rg measurement was performed to measure the compactness of apo form, Bio-0357, and Bio-0597 ligands with spike protein complex structures. As shown in Fig. 4(c), while the apo form Rg value during 10 ns formed a stable curve between 4.75 nm and 5.00 nm, Bio-0597 created an increasing acceleration from 4.75 nm to 5.42 nm, while Bio-0357 produced an acceleration that decreased from 4.82 nm to 4.42 nm. If we look at molecular dynamics studies in general, according to RMSD, RMSF, and Rg analysis Bio-0357 and SARS CoV-2 protein form a stable molecular interaction. MD simulations of zidovudine showed a very stable interaction with fluctuation starting at 2.4 Å on 2 ns and remained stable at 3 Å from 13 to 50 ns with SARS-CoV-2 target proteins of PDB ID:6VYO [20].

Also, the analysis of the number of H bonds that Bio-0357 and Bio-0597 formed with SARS CoV-2 spike glycoprotein at a distance of 3.5 Å (0.35 nm) during 10 ns was performed. As shown in Fig. 4 (d), the Bio-0357 compound formed 2 or 3H bonds during about 7 ns and Bio-0597 rarely formed 1H bond. Bio-0357 compound tends to form more H bonds than Bio-0597. It can be said that Bio-375 interacted with the SARS CoV-2 spike glycoprotein with higher stability than Bio-0597. MD simulations studies showed that all the three complexes of 6VYO with alizarin, aloe-emodin and anthrarufin were stable up to 50 ns with good binding affinities [23].

3.5. Chemical and spectroscopic interactions of protozide/chrysin with F/G systems

Fig. 5 shows optimized protozide-F/G and chrysin-F/G structures. After optimization, protozide get adsorbed nearly perpendicular to F/G clusters (Fig. 5) while chrysin gets nearly parallel to F and nearly perpendicular to G clusters. Adsorption energy is measured by subtracting from the total energy of the combined system, protozide/chrysin over F/G clusters, the amount of individual energy of protozide/chrysin and F/G. Adsorption energies are −15.16/−16.35 kcal/mol for protozide-F/G and −16.52/−17.63 kcal/mol for chrysin-F/G systems [47]. For p-acetanisidide and 4-(3-chloropropoxy)acetanilide, the adsorption energies are reported as −11.17 and −13.64 kcal/mol with graphene and as −11.30 and −13.62 kcal/mol with fullerene systems [48]. In the case of letrozole/metronidazole, the adsorption energies with graphene and fullerene nanoclusters are respectively, −4.5808/-3.8905 kcal/mol and 1.8198/-1.1295 kcal/mol [49]. We explored FMOs (Fig. 6) of protozide-F/G and chrysin-F/G to study binding affinity between protozide/chrysin-F/G and F/G. In Fig. 6: HOMO is over the entire molecule, except pyridine ring and LUMO over the entire molecule except one OH for protozide; HOMO and LUMO over the fullerene with the interchange of orbitals for protozide-F and HOMO over

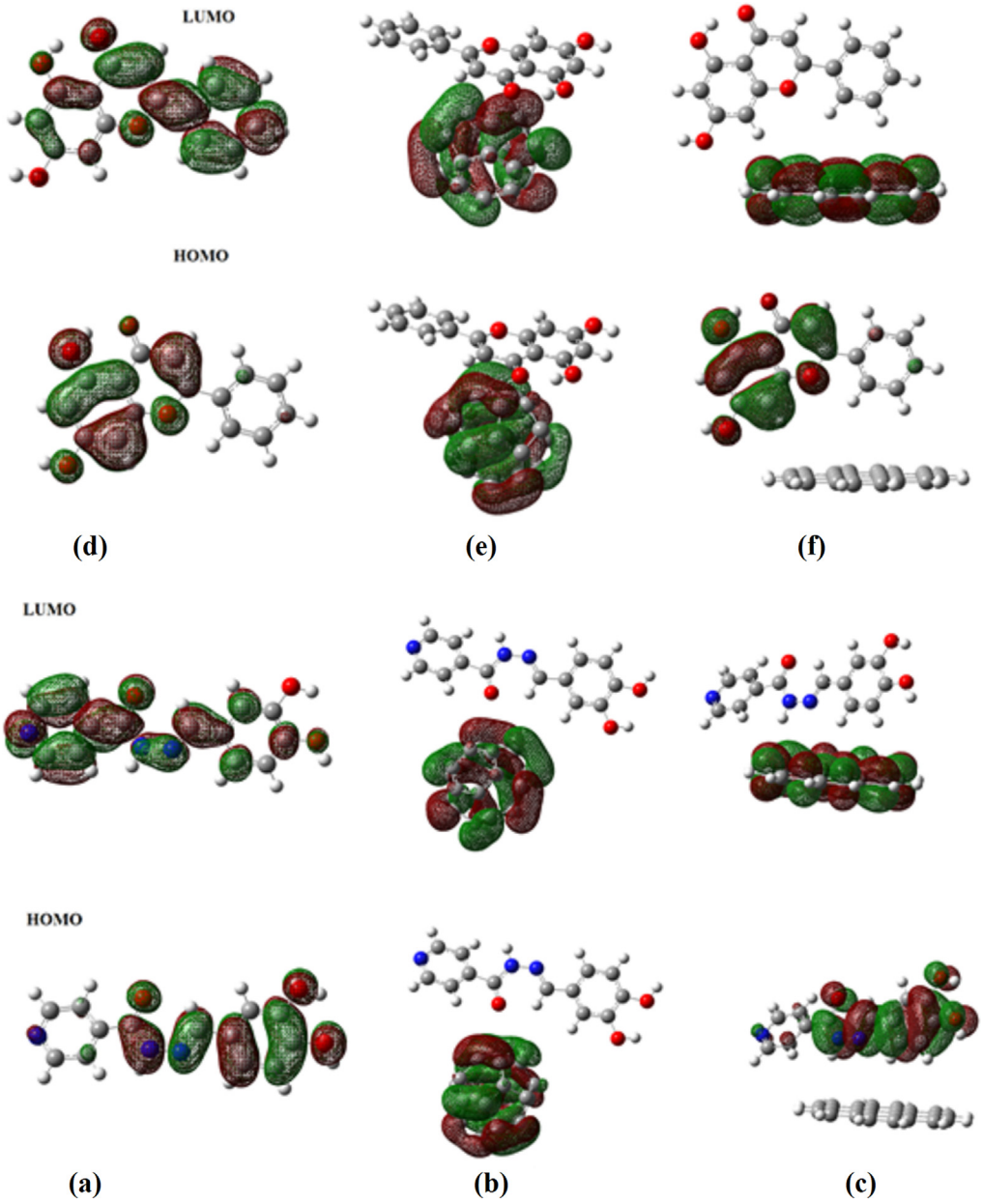

Fig. 6. HOMO-LUMO plots of (a) protozide (b) protozide-F (c) protozide-G (d) chrysin (e) chrysin-F (f) chrysin-G.

the entire protozide molecule except for pyridine and graphene while LUMO is over the graphene only. In Fig. 6: HOMO is over the entire molecule except mono-substituted phenyl ring and LUMO is over the entire molecule for chrysin; HOMO and LUMO are over the fullerene for chrysin-F system and HOMO is over chrysin except for mono-substituted phenyl ring and LUMO is over the graphene alone for the chrysin-G system. HOMO and LUMO delocalization for all systems resulting in charge transfer and different enhancements due to adsorption [50].

HOMO-LUMO gaps (Table S2) of protozide/chrysin over F/G are less than that of pristine values (2.5100/3.0030 eV) with the least value for F systems. These changes in Eg of protozide/chrysin over all F/G show charge transfer. The chemical potential of protozide/chrysin (-6.5848/-7.0117 eV) doped with F/G becomes more negative and electrophilicity values are very high, for F cages which show the bioactivity clusters as nano-drug carriers [51].

In MEP (Fig. 7 for protozide and chrysin systems), red and blue regions are electrophilic and nucleophilic [52]. Red gives negative potential where positive charges are strongly bound and vice versa for blue. For protozide/chrysin adsorbed on F/G, charges of O and N atoms change due to the adsorption process (Table S3) and these changes in charge confirm the enhancement.

The first order hyperpolarizability ($\times 10^{-30}$esu) of protozide/chrysin are 39.285/9.325 while that with fullerene are 44.686/25.518. The second order values ($\times 10^{-37}$esu) are −43.161/-53.766 for chrysin-F/G and −52.581/-55.271 for protozide-F/G. The first-order hyperpolarizability of protozide/chrysin-F is greater than that of pristine molecules. Large enhancement of the second hyperpolarizability of all protozide/chrysin-F/G shows high NLO properties (Table S4). The polarizability also shows enhancement [53]. The first order ($\times 10^{-30}$ esu) and second order ($\times 10^{-37}$ esu) hyperpolarizabilities of letrozole/metronidazole are 2.296/4.421 and –22.537/-4.777 respectively [49].

For letrozole/metronidazole adsorption in graphene/fullerene nanoclusters, the polarizability values are reported as: first order hyperpolarizability ($\times 10^{-30}$ esu), 2.296/4.421 for letrozole/

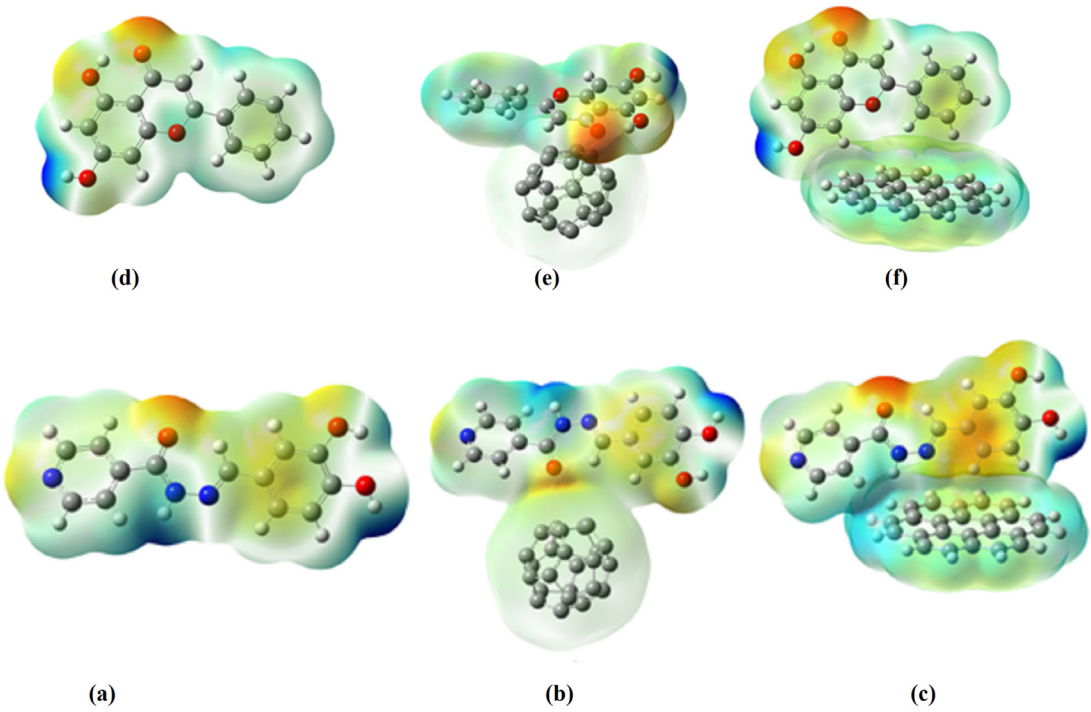

Fig. 7. MEP plots of (a) protozide (b) protozide-F (c) protozide-G (d) chrysin (e) chrysin-F (f) chrysin-G.

metronidazole, 3.713/6.048 and 4.163/10.881 for letrozole/metronidazole graphene and fullerene complexes [49]. The second hyperpolarizability values ($\times 10^{-37}$ esu), for letrozole/letrozole-G/letrozole-F and metronidazole/metronidazole-G/metronidazole-F systems are respectively −22.537/−55.922/−67.560 and −4.777/−45.330/−41.332 [49].

Figs. S6 and S7 show the Raman spectra of protozide and chrysin molecules and with F/G systems. For all QDs, there is an increase in intensity for different modes of protozide/chrysin [54].

4. Conclusion

The present study was carried out to explore potential ligands interaction with newly hypothesized binding sites of ACE2 and TMPRSS2 on S1 and S2 domain of trimeric spike protein of SARS coronavirus-2. A total of 1503 tautomer's of bioactive compounds were used forvirtual screening and docking with three active binding sites on the S1 and S2 domain of spikes protein. Molecular dynamics (MD) simulation was performed for 10 ns to validate the stability behavior of Bio-0357 (Protozide), and Bio-597 (Chrysin) bioactive compounds with S1 binding site of the spike protein. The RMSD, RMSF, and Rg analysis of Bio-0357 and Bio-597 compounds with spike protein forms a stable ligand–protein interaction. *In-silico* docking and dynamic simulations study of both bioactive compounds show good binding affinity (docking score −9.642 and −8.78 kcal/mol with S1 domain and −5.83 and −5.30 kcal/mol), and stable molecular interaction with both target binding sites which can lead to thedevelopment of potential therapeutic drug candidates for preventing the entry of SARS CoV-2 into the human host cell via ACE2 and TMPRSS2 interaction.

The adsorption of protozide/chrysin on F/G has been investigated through DFT simulations. At adsorption of protozide/chrysin, the band gap of protozide/chrysin-F/G is reduced significantly. From SERS results it can be concluded that QDs nanoclusters will act as a sensor for the detection of drugs. The molecular and predictive biological properties of Bio-0357 (Protozide), and Bio-597 (Chrysin) may be helpful for researchers in further experimental validation through in vitro and *in vivo* studies.

CRediT authorship contribution statement

Rohitash Yadav: Conceptualization, Data curation, Formal analysis, Writing-original draft, validation, writing- review and editing, supervision. **Shazia Hasan:** Conceptualization, Data curation, Formal analysis, Writing-original draft, validation, writing- review and editing, supervision. **Sumit Mahato:** Conceptualization, Data curation, Formal analysis, Writing-original draft, validation, writing- review and editing, supervision. **Ismail Celik:** Methodology, Investigation, Resources, Software, Formal analysis, Writing-original draft, review and editing, supervision. **Y. S. Mary:** Methodology, Investigation, Resources, Software, Formal analysis, Writing-original draft, review and editing, supervision. **Ashish Kumar:** Methodology, Investigation, Resources, Software, Formal analysis, Writing-original draft, review and editing, supervision. **Puneet Dhamija:** Methodology, Investigation, Resources, Software, Formal analysis, Writing-original draft, review and editing, supervision. **Ambika Sharma:** Formal analysis, Writing-original draft, review and editing. **Neha Choudhary:** Formal analysis, Writing-original draft, review and editing. **Pankaj Kumar Chaudhary:** Formal analysis, Writing-original draft, review and editing. **Ankita Singh Kushwah:** Formal analysis, Writing-original draft, review and editing. **Jitendra Kumar Chaudhary:** Formal analysis, Writing-original draft, review and editing.

Declaration of Competing Interest

The authors declare that they have no known competing financial interests or personal relationships that could have appeared to influence the work reported in this paper.

Acknowledgments

Thanks to the Department of Pharmacology, All India Institute of Medical Sciences, Rishikesh, and Molecules of Life research lab, Society of Young Biomedical Scientists, India for providing the facility. All molecular dynamics simulations were performed by TÜBİTAK (The Scientific and Technological Research Council of Turkey) ULAKBİM (Turkish Academic Network and Information Centre), High Performance and Grid Computing Centre (TRUBA resources).

Ethical statement

Not applicable.

Funding

Self-funded

Authors' contribution

RY, IS, and YSM designed, supervised, performed, analyzed and wrote the study. SH, SM, AK, NC, ASK, contributed to the writing, editing, and analysis. PD, AS, PKC, SH and JKC reviewed and edited the manuscript.

Appendix A. Supplementary material

Supplementary data to this article can be found online at https://doi.org/10.1016/j.molliq.2021.116942.

References

[1] J. She, J. Jiang, L. Ye, L. Hu, C. Bai, Y. Song, 2019 novel coronavirus of pneumonia in Wuhan, China: emerging attack and management strategies, Clin. Transl. Med. 9 (2020) 19, https://doi.org/10.1186/s40169-020-00271-z.
[2] A.A. Rabaan, S.H. Al-Ahmed, S. Haque, R. Sah, R. Tiwari, Y.S. Malik, et al., SARS-CoV-2, SARS-CoV, and MERS-COV: A comparative overview, Infez. Med. 28 (2020) 174–184.
[3] J. Zheng, SARS-CoV-2: an Emerging Coronavirus that Causes a Global Threat, Int. J. Biol. Sci. 16 (2020) 1678–1685, https://doi.org/10.7150/ijbs.45053.
[4] Y. Roussel, A. Giraud-Gatineau, M.T. Jimeno, J.M. Rolain, C. Zandotti, P. Colson, D. Raoult, SARS-CoV-2: fear versus data, Int. J. Antimicrob. Agents 55 (2020), https://doi.org/10.1016/j.ijantimicag.2020.105947 105947.
[5] F.A. Rabi, M.S. Al Zoubi, G.A. Kasasbeh, D.M. Salameh, A.D. Al-Nasser, SARS-CoV-2 and Coronavirus Disease 2019: What We Know So Far, Pathogens 9 (2020) 231, https://doi.org/10.3390/pathogens9030231.
[6] Eurosurveillance Editorial Team, Note from the editors: World Health Organization declares novel coronavirus (2019-nCoV) sixth public health emergency of international concern, Euro. Surveill. 25 (2020) 200131e, https://doi.org/10.2807/1560-7917.ES.2020.25.5.200131e.
[7] J. Cui, F. Li, Z.L. Shi, Origin and evolution of pathogenic coronaviruses, Nat. Rev. Microbiol. 17 (2019) 181–192, https://doi.org/10.1038/s41579-018-0118-9.
[8] J.F. Chan, K.H. Kok, Z. Zhu, H. Chu, K.K. To, S. Yuan, K.Y. Yuen, Genomic characterization of the 2019 novel human-pathogenic coronavirus isolated from a patient with atypical pneumonia after visiting Wuhan, Emerg. Microbes. Infect. 9 (2020) 221–236, https://doi.org/10.1080/22221751.2020.1719902.
[9] C.I. Paules, H.D. Marston, A.S. Fauci, Coronavirus Infections-More Than Just the Common Cold, JAMA 323 (2020) 707–708, https://doi.org/10.1001/jama.2020.0757.
[10] I. Astuti, X. Ysrafil, Severe Acute Respiratory Syndrome Coronavirus 2 (SARS-CoV-2): An overview of viral structure and host response, Diabetes Metab. Syndr. 14 (2020) 407–412, https://doi.org/10.1016/j.dsx.2020.04.020.
[11] J.-H. Won, H. Lee, The current status of drug repositioning and vaccine developments for the COVID-19 pandemic, Int. J. Mol. Sci. 21 (2020) 9775, https://doi.org/10.3390/ijms21249775.
[12] C. Wu, Y. Liu, Y. Yang, P. Zhang, W. Zhong, Y. Wang, et al., Analysis of therapeutic targets for SARS-CoV-2 and discovery of potential drugs by computational methods, Acta Pharm. Si.n B 10 (2020) 766–788, https://doi.org/10.1016/j.apsb.2020.02.008.
[13] O.V. de Oliveira, G.B. Rocha, A.S. Paluch, L.T. Costa, Repurposing approved drugs as inhibitors of SARS-CoV-2 S-protein from molecular modeling and virtual screening, J. Biomol. Struct. Dyn. (2020) 1–10, https://doi.org/10.1080/07391102.2020.1772885.
[14] A.B. Durojaiye, J.D. Clarke, G.A. Stamatiades, C. Wang, Repurposing cefuroxime for treatment of COVID-19: a scoping review of, J. Biomol. Struct. Dyn. (2020) 1–8, https://doi.org/10.1080/07391102.2020.1777904.
[15] S.A. Amin, S. Banerjee, K. Ghosh, S. Gayen, T. Jha, Protease targeted COVID-19 drug discovery and its challenges: Insight into viral main protease (Mpro) and papain-like protease (PLpro) inhibitors, Bioorg. Med. Chem. 29 (2020), https://doi.org/10.1016/j.bmc.2020.115860 115860.
[16] D.H. Zhang, K.L. Wu, X. Zhang, S.Q. Deng, B. Peng, In silico screening of Chinese herbal medicines with the potential to directly inhibit 2019 novel coronavirus, J. Integr. Med. 18 (2020) 152–158, https://doi.org/10.1016/j.joim.2020.02.005.
[17] I. Aanouz, A. Belhassan, K. El-Khatabi, T. Lakhlifi, M. El-Ldrissi, M. Bouachrine, Moroccan Medicinal plants as inhibitors against SARS-CoV-2 main protease: Computational investigations, J. Biomol. Struct. Dyn. (2020) 1–9, https://doi.org/10.1080/07391102.2020.1758790.
[18] R. Yadav, M. Imran, P. Dhamija, D.K. Chaurasia, S. Handu, Virtual screening, ADMET prediction and dynamics simulation of potential compounds targeting the main protease of SARS-CoV-2, J. Biomol. Struct. Dyn. (2020) 1–16, https://doi.org/10.1080/07391102.2020.1796812.
[19] M. Miczi, M. Golda, B. Kunkli, T. Nagy, J. Tőzsér, J.A. Mótyán, Identification of Host Cellular Protein Substrates of SARS-COV-2 Main Protease, Int. J. Mol. Sci. 21 (2020) 9523, https://doi.org/10.3390/ijms21249523.
[20] R. Yadav, M. Imran, P. Dhamija, K. Suchal, S. Handu, Virtual screening and dynamics of potential inhibitors targeting RNA binding domain of nucleocapsid phosphoprotein from SARS-CoV-2, J. Biomol. Struct. Dyn. (2020) 1–16, https://doi.org/10.1080/07391102.2020.1778536.
[21] Z. Zehra, M. Luthra, S.M. Siddiqui, A. Shamsi, N.A. Gaur, A. Islam, Corona virus versus existence of human on the earth: A computational and biophysical approach, Int. J. Biol. Macromol. 161 (2020) 271–281, https://doi.org/10.1016/j.ijbiomac.2020.06.007.
[22] S. Kandwal, D. Fayne, Repurposing drugs for treatment of SARS-CoV-2 infection: computational design insights into mechanisms of action, J. Biomol. Struct. Dyn. (2020) 1–15, https://doi.org/10.1080/07391102.2020.1825232.
[23] R. Rolta, R. Yadav, D. Salaria, S. Trivedi, M. Imran, A. Sourirajan, D.J. Baumler, K. Dev, screening of hundred phytocompounds of ten medicinal plants as potential inhibitors of nucleocapsid phosphoprotein, J. Biomol. Struct. Dyn. (2020) 1–18, https://doi.org/10.1080/07391102.2020.1804457.
[24] F. Li, Structure, Function, and Evolution of Coronavirus Spike Proteins, Annu. Rev. Virol. 3 (2016) 237–261, https://doi.org/10.1146/annurev-virology-110615-042301.
[25] J. Lan, J. Ge, J. Yu, S. Shan, H. Zhou, S. Fan, et al., Structure of the SARS-CoV-2 spike receptor-binding domain bound to the ACE2 receptor, Nature 581 (2020) 215–220, https://doi.org/10.1038/s41586-020-2180-5.
[26] M. Hoffmann, H. Kleine-Weber, S. Schroeder, N. Krüger, T. Herrler, S. Erichsen, et al., SARS-CoV-2 Cell Entry Depends on ACE2 and TMPRSS2 and Is Blocked by a Clinically Proven Protease Inhibitor, Cell 181 (2020) 271–280, https://doi.org/10.1016/j.cell.2020.02.052.
[27] Z. Jafari, R. Baharfar, A.S. Rad, S. Asghari, Potential of graphene oxide as a drug delivery system of sumatriptan, A detailed density functional theory study, J. Biomol. Struct. Dyn. 39 (2021) 1611–1620, https://doi.org/10.1080/07391102.2020.1736161.
[28] J.S. Al-Otaibi, Y.S. Mary, Y.S. Mary, S. Kaya, S. Erkan, Spectral analysis and DFT investigation of some benzopyran analogues and their self assemblies with graphene, J. Mol. Liq. 317 (2020), https://doi.org/10.1016/j.molliq.2020.113924 113924.
[29] R. Padash, M.R. Esfahani, A.S. Rad, The computational quantum mechanical study of sulfamide drug adsorption onto X12Y12 fullerene like nanocages: Detailed DFT and QYAIM investigations, J. Biomol. Struct. Dyn. (2020), https://doi.org/10.1080/07391102.2020.1792991.
[30] G.M. Sastry, M. Adzhigirey, T. Day, R. Annabhimoju, W. Sherman, Protein and ligand preparation: parameters, protocols, and influence on virtual screening enrichments, J. Comput. Aided Mol. Des. 27 (2013) 221–234, https://doi.org/10.1007/s10822-013-9644-8.
[31] T.A. Halgren, Identifying and characterizing binding sites and assessing druggability, J. Chem. Inf. Model. 49 (2009) 377–389, https://doi.org/10.1021/jm030644s.
[32] G. Lanka, R. Bathula, M. Dasari, S. Nakkala, M. Bhargavi, G. Somadi, S.R. Potlapally, Structure-based identification of potential novel inhibitors targeting FAM3B (PANDER) causing type 2 diabetes mellitus through virtual screening, J. Recept. Signal Transduct. Res. 39 (2019) 253–263, https://doi.org/10.1080/10799893.2019.1660897.
[33] T.A. Halgren, R.B. Murphy, R.A. Friesner, H.S. Beard, L.L. Frye, W.T. Pollard, J.L. Banks, Glide: a new approach for rapid, accurate docking and scoring. 2. Enrichment factors in database screening, J. Med. Chem. 47 (2004) 1750–1759, https://doi.org/10.1021/jm030644s.
[34] K.G. Tina, R. Bhadra, N.P.I.C. Srinivasan, Protein Interactions Calculator, Nucleic Acids Res. 35 (Web Server issue) (2007) W473–476, https://doi.org/10.1093/nar/gkm423.
[35] B. Kohnke, C. Kutzner, H. Grubmüller, A GPU-Accelerated Fast Multipole Method for GROMACS: Performance and Accuracy, J. Chem. Theory. Comput. 16 (2020) 6938–6949, https://doi.org/10.1021/acs.jctc.0c00744.
[36] N. Guex, M.C. Peitsch, SWISS-MODEL and the Swiss-PdbViewer: an environment for comparative protein modeling, Electrophoresis 18 (1997) 2714–2723, https://doi.org/10.1002/elps.1150181505.

[37] J. Huang, A.D. MacKerell, CHARMM36 all-atom additive protein force field: validation based on comparison to NMR data, J. Comput. Chem. 34 (2013) 2135–2145, https://doi.org/10.1002/jcc.23354.
[38] M.J. Frisch, G.W. Trucks, H.B. Schlegel, G.E. Scuseria, M.A. Robb, J.R. Cheeseman, G. Scalmani, V. Barone, B. Mennucci, G.A. Petersson, H. Nakatsuji, M. Caricato, X. Li, H.P. Hratchian, A.F. Izmaylov, J. Bloino, G. Zheng, J.L. Sonnenberg, M. Hada, M. Ehara, K. Toyota, R. Fukuda, J. Hasegawa, M. Ishida, T. Nakajima, Y. Honda, O. Kitao, H. Nakai, T. Vreven, J.A. Montgomery Jr., J.E. Peralta, F. Ogliaro, M. Bearpark, J.J. Heyd, E. Brothers, K.N. Kudin, V.N. Staroverov, T. Keith, R. Kobayashi, J. Normand, K. Raghavachari, A. Rendell, J.C. Burant, S.S. Iyengar, J. Tomasi, M. Cossi, N. Rega, J.M. Millam, M. Klene, J.E. Knox, J.B. Cross, V. Bakken, C. Adamo, J. Jaramillo, R. Gomperts, R.E. Stratmann, O. Yazyev, A.J. Austin, R. Cammi, C. Pomelli, J.W. Ochterski, R.L. Martin, K. Morokuma, V.G. Zakrzewski, G.A. Voth, P. Salvador, J.J. Dannenberg, S. Dapprich, A.D. Daniels, O. Farkas, J.B. Foresman, J. Ortiz, J. Cioslowski, D.J. Fox, Gaussian 09, Revision D.01, Gaussian, Inc., Wallingford CT, 2013.
[39] R. Dennington, T. Keith, J. Millam, Semichem Inc, Shawnee Mission KS, GaussView, 2009.
[40] A.H. Almuqrin, J.S. Al-Otaibi, Y.S. Mary, Y.S. Mary, R. Thomas, Structural study of letrozole and metronidazole and formation of self-assembly with graphene and fullerene with the enhancement of physical, chemical and biological activities, J. Biomol. Struct. Dyn. (2020), https://doi.org/10.1080/07391102.2020.1790420.
[41] R.A. Laskowski, J.A. Rullmannn, M.W. MacArthur, R. Kaptein, J.M. Thornton, AQUA and PROCHECK-NMR: programs for checking the quality of protein structures solved by NMR, J. Biomol. NMR 8 (1996) 477–486, https://doi.org/10.1007/BF00228148.
[42] T.E. Tallei, S.G. Tumilaar, N.J. Niode, Fatimawali, B.J. Kepel, R. Idroes, Y. Effendi, S.A. Sakib, T.B. Emran, Potential of plant bioactive compounds as SARS-CoV-2 main protease (Mpro) and spike (S) glycoprotein inhibitors: A molecular docking study, Scientifica (2020) 6307457, https://doi.org/10.1155/2020.6307457.
[43] A. Basu, A. Sarkar, U. Maulik, Molecular docking study of potential phytochemicals and their effects on the complex of SARS-CoV2 spike protein and human ACE2, Sci. Rep. 10 (2020) 17699, https://doi.org/10.1038/s41598-020-74715-4.
[44] S. Lehrer, P.H. Rheinstein, Ivermectin docks to the SARS-CoV-2 spike receptor-binding domain attached to ACE2, Vivo 34 (2020) 3023–3026, https://doi.org/10.21873/invivo.12134.
[45] A.F. Eweas, A.A. Alhossary, A.S. Abdel-Moneim, Molecular docking reveals ivermectin and remdesivir as potential repurposed drugs against SARS-CoV-2, Front. Microbiol. 11 (2021), https://doi.org/10.3389/fmicb.2020.592908 592908.
[46] X.D. Wu, B. Shang, R.F. Yang, H. Yu, Z.H. Ma, X. Shen, et al., spike protein of severe acute respiratory syndrome (SARS) is cleaved in virus infected Vero-E6 cells, Cell Res. 14 (2004) 400–406, https://doi.org/10.1038/sj.cr.7290240.
[47] J.D. Wuest, A. Rochefort, Strong adsorption of aminotriazines on graphene, Chem. Commun. 46 (2010) 2923–2925, https://doi.org/10.1039/B926286E.
[48] A.H. Almuqrin, J.S. Al-Otaibi, Y.S. Mary, R. Thomas, S. Kaya, D.O. Isin, Spectral analysis and detailed quantum mechanical investigation of some acetanilide analogues and their self-assemblies with graphene and fullerene, J. Mol. Model. 26 (2020) 254, https://doi.org/10.1007/s00894-020-04485-3.
[49] A.H. Almuqrin, J.S. Al-Otaibi, Y.S. Mary, Y.S. Mary, R. Thomas, Structural study of letrozole and metronidazole and formation of self-assembly with graphene and fullerene with the enhancement of physical, chemical and biological activities, J. Biomol. Struct. Dyn. (2020), https://doi.org/10.1080/07391102.2020.17905420.
[50] J.S. Al-Otaibi, Y.S. Mary, R. Thomas, S. Kaya, Detailed electronic structure, physic chemical properties, excited state properties, virtual bioactivity screening and SERS analysis of three guanine based antiviral drugs, valacyclovir HCl hydrate, Acyclovir and ganciclovir, Polycyc. Aromat. Comp. (2020), https://doi.org/10.1080/10406638.2020.1773876.
[51] C.S.C. Kumar, C.Y. Panicker, H.K. Fun, Y.S. Mary, B. Harikumar, S. Chandraju, C. K. Quah, C.W. Ooi, FT-IR, molecular structure, first order hyperpolarizability, HOMO and LUMO analysis, MEP and NBO analysis of 2-(4-chlorophenyl)-2-oxoethyl 3-nitrobenzoate, Spectrochim. Acta 126 (2014) 208–219, https://doi.org/10.1016/j.saa.2014.01.145.
[52] M. Hossain, R. Thomas, Y.S. Mary, K.S. Resmi, S. Armakovic, S.J. Armakovic, A.K. Nanda, G. Vijayakumar, C. Van Alsenoy, Understanding reactivity of two newly synthetized imidazole derivatives by spectroscopic characterization and computational study, J. Mol. Struct. 1158 (2018) 176–196, https://doi.org/10.1016/j.molstruc.2018.01.029.
[53] Y.S. Mary, H.T. Varghese, C.Y. Panicker, M. Girisha, B.K. Sagar, H.S. Yathirajan, A. A. Al-Saadi, C. Van Alsenoy, Vibrational spectra, HOMO, LUMO, NBO, MEP analysis and molecular docking study of 2,2-diphenyl-4-(piperidin-1yl) butanamide, Spectrochim. Acta 150 (2015) 543–556, https://doi.org/10.1016/j.saa.2015.05.090.
[54] Y.S. Mary, Y.S. Mary, Utilization of doped/undoped graphene quantum dots for ultrasensitive detection of duphaston, a SERS platform, Spectrochim. Acta 244 (2021), https://doi.org/10.1016/j.saa.2020.118865 118865.